

Tracking of Gaussian pulse release length inside mode-locked semiconductor laser amplifier

Mubarak Hamad Oglah, Watban Ibrahim Mahmood, Nawras Basheer Adday

Department of Mechanical Engineering, College of Shirgat Engineering, Tikrit University, Tikrit, Iraq

Article Info

Article history:

Received Sep 17, 2022

Revised Jun 14, 2023

Accepted Jul 8, 2023

Keywords:

Electric field
Gaussian pulse
Mode locked
Pulse duration
Semiconductor laser

ABSTRACT

The behavior of the optical pulse release was investigated during chirped pulses amplification, which consisted of two chirped fiber Bragg grating and one semiconductor optical amplifier (SOA). This occurred when the pulse width, (τ_p) \ll carrier lifetime (τ_c), as well as the effect of the length parameter on the shape and spectrum of the electric field, intensity, and phase of amplified pulses, were taken into consideration. The purpose of this research is to investigate the effect of release length on the temporal electric field laser amplifier while simultaneously generating optical pulses with the help of a mode-locked laser system semiconductor. In the scenario where τ_p and τ_c are taken into account, we discovered that the length of the release has a significant impact on the modes of the phase and the electric field.

This is an open access article under the [CC BY-SA](https://creativecommons.org/licenses/by-sa/4.0/) license.



Corresponding Author:

Mubarak Hamad Oglah

Department of Mechanical Engineering, College of Shirgat Engineering, Tikrit University

500 Algadsia, Iraq

Email: mubarak@tu.edu.iq

1. INTRODUCTION

In order for the laser system to be functional in a variety of laser applications, such as laser radar, material processing, non-linear frequency conversion, and others, its specifications need to be met. Power, optical spectrum quality, optical pulse width, and spatial beam type are examples of typical requirements [1]–[3]. Because the output power that was directly derived from the laser oscillator was insufficient for many purposes, the output power of the laser oscillator had to be increased in order to fulfill the requirements of those applications. Following the laser oscillator was an optical magnifier that was utilized [4]–[6]. The device that included both a laser oscillator and an optical amplifier in a single package. It was determined how to calculate spectral width, optical pulse shape, and beam spacing; nonetheless, the power amplifier was responsible for calculating pulse power [7], [8].

When it came to semiconductor lasers, the optical resonator was responsible for defining the optical field and, as a result, increasing the optical amplification that resulted from stimulated emission [9]–[11]. In order to the implementation of the one-dimensional resonator was done in order to keep the light field contained within the laser cavity. This required the utilization of two mirrors, each of which only partially reflected the surrounding environment. The output of the observed laser was light that was transmitted. This was because the reflecting mirrors only allowed a small percentage of the light to pass through them. These mirrors are what generate a Fabry-Perot resonance of the electromagnetic field in common laser designs; this is necessary in order to get the laser to its steady state [12], [13]. There were quite a few resonances in the Fabry-Beirut cavity. A frequency comb, also known as modes, was produced as a result of those patterns, and it was located at the frequency of the Fabry-Beirut cavity's round-trip. Only one or a few of these modes existed in the steady laser state above the threshold limit [14]. This is because the gain bandwidth in the active laser region was rather

narrow. In the majority of cases, there was no connection between these phases [15], [16]. These factors led to a laser output that was rather consistent [17], [18], while having a random distribution in time. The light output was a succession of successive pulses whenever the phases of these modes were placed in close proximity to one another to reduce the likelihood of them colliding with one another. This was because the inverse Fourier transform of equal-frequency pulses was fundamentally an infinite train of pulses in the time domain. This was the reason for this phenomenon. This was the reason why everything that took place was due to this. These genetic modifications of the time domain, which correlate to the light pulses [19], [20]. In this study, we will investigate the influence that the length of the tracking parameter has on the form and temporary electric field distribution of a laser mode-locked system where the pulse width (τ_p) is greater than the carrier lifetime (τ_c) both before and after the amplification process.

2. METHOD

The paper known Figure 1 was the one that presented the fundamental framework of the model. Lee and Delfyett [21], Hillbrand *et al.* [22], and Pimenov *et al.* [23] were aware with the concept of pulse propagation inside amplifiers after determining that the pulse width, t , is less than 25 Ps. This theory was useful for analyzing amplifiers as systems consisting of two energy levels, such as gas and solid-state amplifiers. This theory can be extended to include semiconductor lasers if the lasers have two energy levels, one of which is represented by the valence beam and the other of which is represented by the conduction beam. If the semiconductor lasers have two energy levels, this theory can be expanded to include semiconductor lasers [24], [25].

In mathematical processors, simplification first appeared when the pulse width was much larger than the slot time of the gap, which caused τ_p to be more than 1. This caused the problem to be simplified [26]. The approximation rate equations were validated under these conditions, and the equation that was utilized to characterize the visual field E was as [27]:

$$\frac{\partial N}{\partial t} = D\nabla^2 N + \frac{I}{qV} - \frac{N}{\tau_c} - \frac{a(N-N_0)}{h\omega_0} |E|^2 \tag{1}$$

where N stood for the carrier density, D stood for the diffusion parameter, q stood for the charge, I stood for the current injection, V stood for the volume, a stood for the gain, c stood for the carrier lifespan, N_0 stood for the transparency, and E was the energy of the photon.

$$\frac{\partial N}{\partial t} = D\nabla^2 N + \frac{I}{qV} - \frac{N}{\tau_c} - \frac{a(N-N_0)}{h\omega_0} |E|^2 \tag{2}$$

Where:

$$P_{out}(\tau) = P_{in}(\tau) \cdot e^{h(\tau)} \tag{3}$$

$$\phi_{out}(\tau) = \phi_{in}(\tau) - \frac{1}{2} \cdot \alpha \cdot h(\tau) \tag{4}$$

P_{in} and ϕ_{in} are the Phase and power inputs.
The equation was:

$$h(\tau) = \int_0^L g(z, \tau) dz \tag{5}$$

to find out if the gain will remain the same throughout the duration of the pulse. We arrived at this conclusion by continuously integrating (4) along the full length and making use of several of the gain equations. At the:

$$\frac{dh}{d\tau} = \frac{g_0 L - h}{\tau_c} - \frac{P_{in}(\tau)}{E_{sat}} [e^{h(\tau)} - 1] \tag{6}$$

one might determine the value h by applying the input pulse and gain to (5), and then solving that (5). In addition, it was possible to ascertain the shape of the pulse as well as its phase. Both the simulation procedure and the parameters were taken into account. Broken down and described in Figure 1 and Table 1.

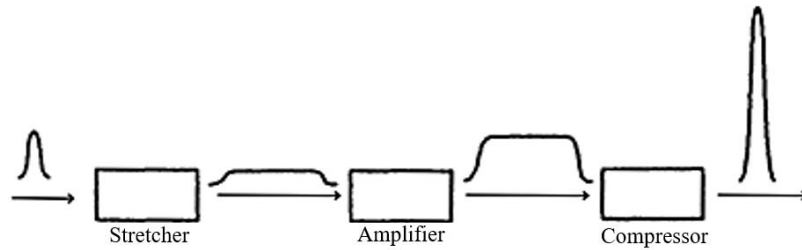


Figure 1. Block diagram of the simulation procedure [28]

Table 1. Parameters used in the simulation

Symbol	Quantity	Value
λ	Center wavelength	975×10^{-9} m
C	Speed light	3×10^8 m/s
E_{in}	Input energy	5×10^{-12} [Joule]
A_{int}	Internal loss	8.86 cm ⁻¹
K	Wave number	$2\pi/\lambda$
E_{sat}	Saturation energy	0.5 pJ
T	Carrier life time	16 ps
Y_g	Group velocity	$c/4$ m/s
L	Total length	0.005 m
LSOA	SOA length	$10-25$ ps/nm
N_0	the transparency	5×10^{15} cm ⁻¹
ϵ	pulse duration	[0.01 ps]

3. RESULTS AND DISCUSSION

The Runge-Kutta method was utilized in order to carry out a numerical solution to the rate equations of the semiconductor laser. In order to calculate the chirping pulse amplification efficiency, a specific optical pulse generated by a mode-locked semiconductor laser was stretched for the purpose of this experiment. Within a semiconductor optical amplifier, a tracking approach was used to model the stretching, and a Bragg grating was used to simulate the pressure of the stretched pulse. The simulation of the stretching was accomplished.

In addition to the spectral amplitude, the calculation also takes into account the output power and the phase. The time dependency of the train pulses, temporal intensity, and temporal phase, as well as the electric field, are depicted in Figure 2. In Figure 2(a), the temporal dependency of the train pulses for an input optical pulse mode-locked semiconductor laser is illustrated. This plot shows the timing of the individual pulses within the pulse train. The spacing between the pulses is typically regular in mode-locked lasers.

Figure 2(b) represents the temporal intensity of the pulse train. It shows the variation in the intensity of the pulses over time. The intensity usually exhibits a periodic pattern corresponding to the repetition rate of the mode-locked laser. Figure 2(c) shows the electric field of the pulse train. The electric field represents the strength and direction of the electromagnetic wave associated with the optical pulses. The plot provides information about the amplitude and phase of the electric field as a function of time.

Moving on to Figure 3, it displays the temporal phase and spectral electric field for a single pulse within the pulse train. The temporal phase represents the variation of the phase of the electric field as a function of time within a single pulse. The spectral electric field describes the frequency content or spectrum of the electric field associated with the pulse. It provides information about the distribution of frequencies present in the pulse. These figures collectively provide insights into the temporal behavior, intensity, electric field, phase, and spectral characteristics of the pulse train and individual pulses in a mode-locked semiconductor laser.

The extended input pulse lasted for a span of time ranging from 200 ps to 10 ns, and the input power increased after each instance of the power saturation condition taking place. A tiny signal gain of 20 dBm was employed for the semiconductor optical amplifier (SOA), along with a saturation energy of 30 pJ and a vector life of 200 seconds. It was discovered that when the duration of the extended input pulse grew longer in time, the 3dB output saturation power of SOA grew longer as well. This led to a higher power output of the SOA saturation power.

The results of the input pulse after passing through the chirped fiber Bragg grating (CFBG) are shown in Figures 3, 4, and 5. The spectrum of the electric field and the temporal intensity at the stretched pulse following the CFBG are both explained by these Figures. The findings made it abundantly evident that the electric field distribution along the gradient line was centered in the central of the wave guide [29]-[31].

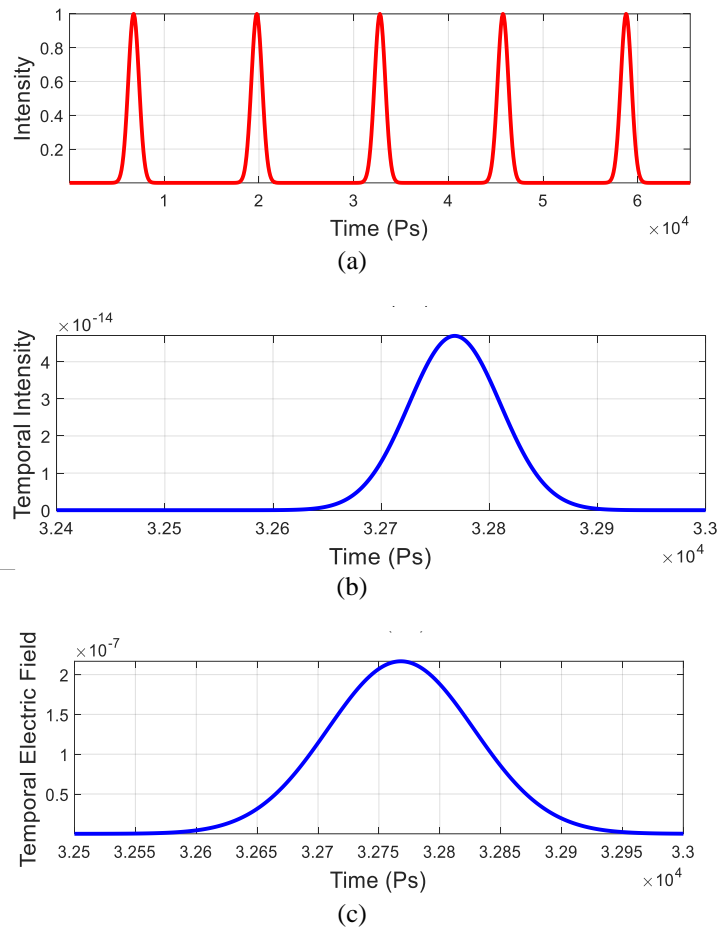


Figure 2. Time dependence of the input optical pulse (a) train pulses, (b) temporal intensity, and (c) temporal electric field

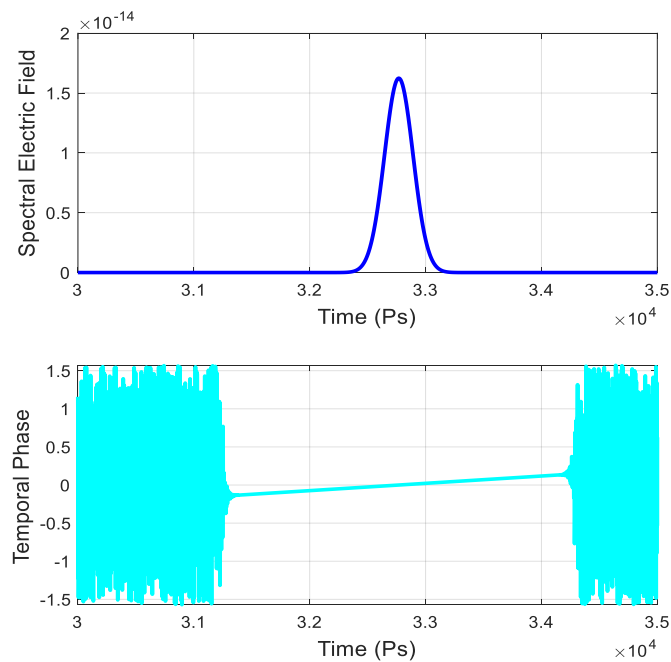


Figure 3. Temporal phase and spectral electric field for the input pulses

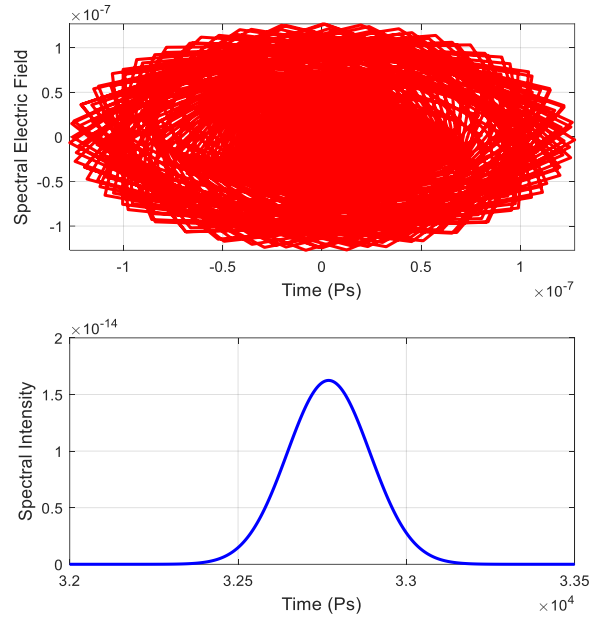


Figure 4. Spectral of the electric field and intensity at stretched pulse after CFBG

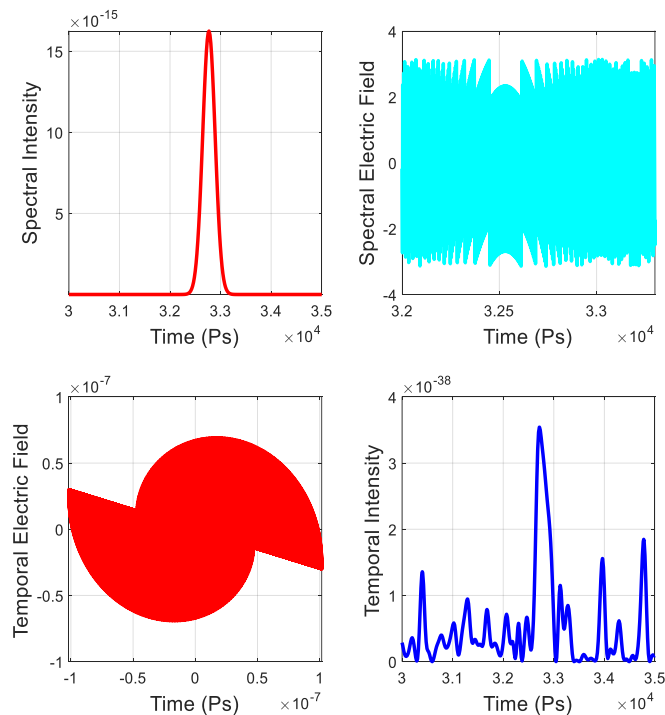


Figure 5. Temporal and intensity of the electric field and intensity at stretched pulse after CFBG

To effectively enter mode-locked, you must first: because the side reflection restricted the bandwidth on the spectrum, selecting the facet reflectivity of the external laser cavity was very critical. Because of this plus the fact that SOA have a very low facet reflectivity (10^{-4}), they have been utilized in mode-locked semiconductor lasers. As a result of certain physical processes, temporal pulse distortion will occur whenever pulse amplification is performed. In the event that the spatial beam distribution was not uniform, since, at greater light intensities, the area inside the optical amplifier operated like a lens, and in case the spatial beam distribution was not uniform. That will result in the optical amplifier becoming compromised. Regular

pumping, irregularity in gain media, diffraction effects, thermal distortions, index nonlinearity, and spatial gain saturation were all well-known physical processes. Figures 6 and 7 illustrate the temporal phase, intensity, electric field, amplitude, and spectral intensity of the amplifier during stretched pulse amplification (SOA).

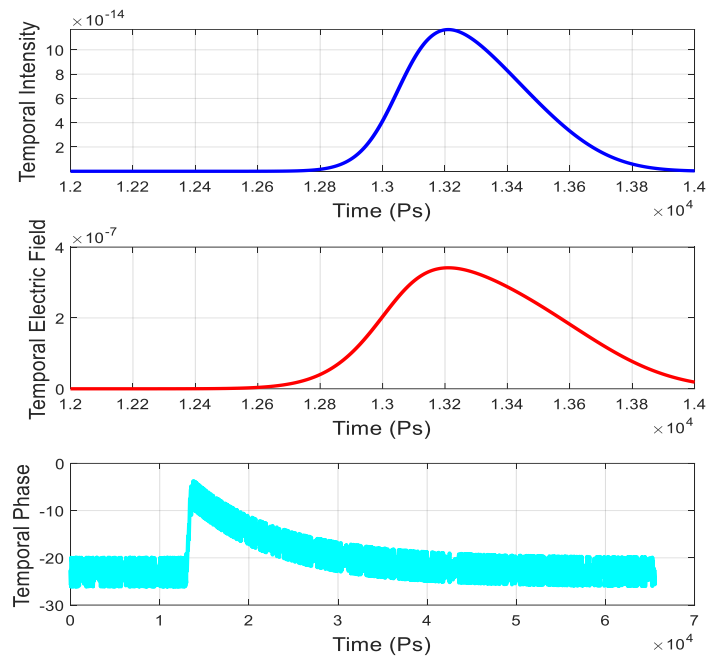


Figure 6. Temple of the phase, intensity, and electric field at amplifying stretched pulse the amplifier

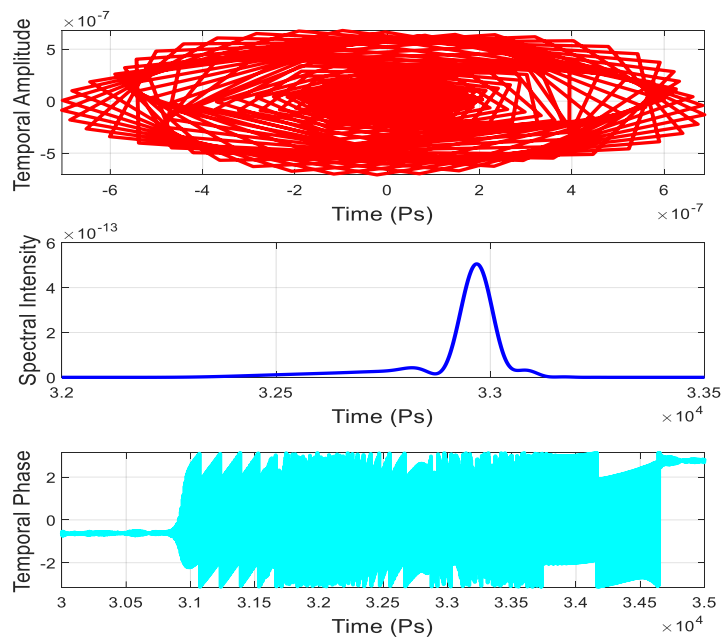


Figure 7. Shows the phase, amplitude, and spectral intensity of the temple of the amplified stretched pulse in the amplifier

The grating compressor was utilized for two different reasons and served two distinct functions inside the system. One of their responsibilities was to make up for the pre-chirping of an optical pulse, which was

produced by an oscillator in a straightforward manner. The other option was to analyze the phase relation of the optical spectrum and access the Fourier plane in order to alter optical spectra that were not desired. Figures 8 and 9 displayed the spectrum intensity, electric field intensity, temporal intensity, and phase of the recompressed pulse that was produced by CFBG.

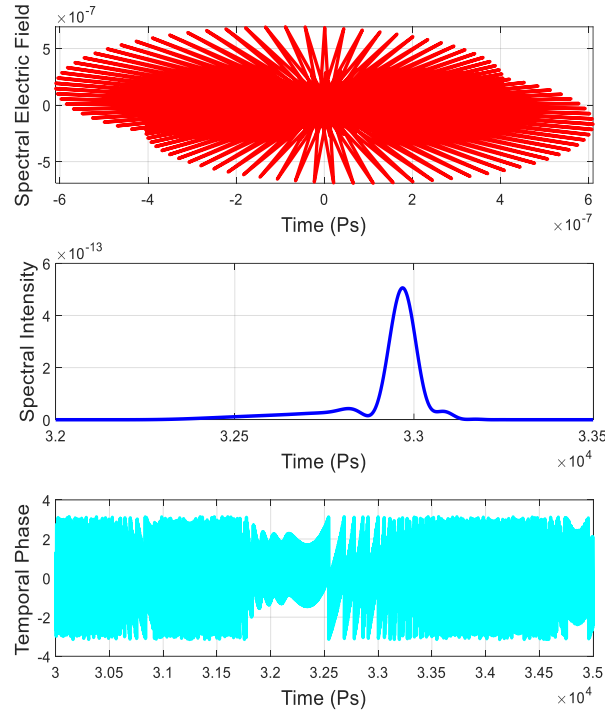


Figure 8. Spectral of the intensity and electric field and temporal phase at recompressed pulse after CFBG

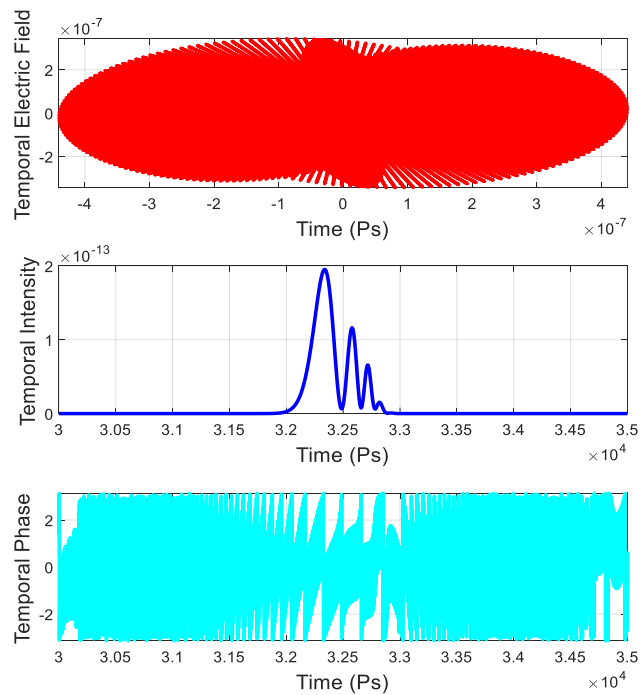


Figure 9. Temporal of the intensity, electric field, and phase at recompressed pulse after CFBG

4. CONCLUSION

It has been looked at how the behavior of the optical pulse tracking changes during the process of chirped pulses amplification when the pulse width and carrier lifetime change. The most important finding was that the duration of the pulse used to inject electric field was a function of the input pulse, particularly for the gain guided of the traveling wave. At addition, the findings of our study demonstrated that the concentration of the electric field distribution across the waveguide can be found in the middle of the gradient line.

ACKNOWLEDGEMENTS

The author is grateful to anonymous rulers for useful comments and suggestions. The Digital Analysis Laboratory partially supports this work.

REFERENCES

- [1] P. M. W. French, "Ultrafast solid-state lasers," *Contemporary Physics*, vol. 37, no. 4, pp. 283–301, Jul. 1996, doi: 10.1080/00107519608222155.
- [2] F. Wang *et al.*, "Short terahertz pulse generation from a dispersion compensated modelocked semiconductor laser," *Laser and Photonics Reviews*, vol. 11, no. 4, p. 1700013, Jul. 2017, doi: 10.1002/apor.201700013.
- [3] F. Zhang *et al.*, "Mode locked Nd³⁺ and Gd³⁺ co-doped calcium fluoride crystal laser at dual gain lines," *Optics and Laser Technology*, vol. 100, pp. 294–297, Mar. 2018, doi: 10.1016/j.optlastec.2017.10.018.
- [4] R. Arkhipov, "Modeling of mode-locking regimes in lasers," Ph.D. dissertation, Mathematisch-Naturwissenschaftlichen Fakultät, Humboldt-Universität zu Berlin, Berlin, 2015.
- [5] A. Bhardwaj *et al.*, "A monolithically integrated racetrack colliding-pulse mode-locked laser with pulse-picking modulator," *IEEE Journal of Quantum Electronics*, vol. 56, no. 4, pp. 1–8, Aug. 2020, doi: 10.1109/JQE.2020.2994990.
- [6] U. Tegin, B. Rahmani, E. Kakkava, D. Psaltis, and C. Moser, "Single-mode output by controlling the spatiotemporal nonlinearities in mode-locked femtosecond multimode fiber lasers," *Advanced Photonics*, vol. 2, no. 5, Oct. 2020, doi: 10.1117/1.AP.2.5.056005.
- [7] R. Häring, R. Paschotta, A. Aschwanden, E. Gini, F. Morier-Genoud, and U. Keller, "High-power passively mode-locked semiconductor lasers," *IEEE Journal of Quantum Electronics*, vol. 38, no. 9, pp. 1268–1275, Sep. 2002, doi: 10.1109/JQE.2002.802111.
- [8] Z. Guo, Q. Hao, J. Peng, and H. Zeng, "Environmentally stable Er-fiber mode-locked pulse generation and amplification by spectrally filtered and phase-biased nonlinear amplifying long-loop mirror," *High Power Laser Science and Engineering*, vol. 7, p. e47, Aug. 2019, doi: 10.1017/hpl.2019.29.
- [9] L. A. Coldren, "Diode lasers and photonic integrated circuits," *Optical Engineering*, vol. 36, no. 2, p. 616, Feb. 1997, doi: 10.1117/1.601191.
- [10] S. Meinecke, L. Drzewietzki, C. Weber, B. Lingnau, S. Breuer, and K. Lüdge, "Ultra-short pulse generation in a three section tapered passively mode-locked quantum-dot semiconductor laser," *Scientific Reports*, vol. 9, no. 1, p. 1783, Feb. 2019, doi: 10.1038/s41598-018-38183-1.
- [11] B. Nyushkov, A. Ivanenko, S. Smirnov, and S. Kobtsev, "High-energy pulses from all-PM ultra-long Yb-fiber laser mode-locked with quasi-synchronous pumping," *Optical Fiber Technology*, vol. 66, p. 102650, Oct. 2021, doi: 10.1016/j.yofte.2021.102650.
- [12] J. Javaloyes and S. Balle, "Mode-locking in semiconductor Fabry-Pérot lasers," *IEEE Journal of Quantum Electronics*, vol. 46, no. 7, pp. 1023–1030, Jul. 2010, doi: 10.1109/JQE.2010.2042792.
- [13] F. Chen, Q. Hao, and H. Zeng, "Optimization of an NALM mode-locked all-PM Er:Fiber laser system," *IEEE Photonics Technology Letters*, vol. 29, no. 23, pp. 2119–2122, Dec. 2017, doi: 10.1109/LPT.2017.2765686.
- [14] J. W. D. Chi, A. Fernandez, and C. Lu, "Properties of mode-locked optical pulses in a dispersion-managed fiber-ring laser using semiconductor optical amplifier as active device," *IEEE Journal of Quantum Electronics*, vol. 49, no. 1, pp. 80–88, Jan. 2013, doi: 10.1109/JQE.2012.2230317.
- [15] F. X. Kaertner, "Ultrafast optical physics II," in *Lecture Notes at the University of Hamburg*, 2014.
- [16] F. Gallazzi *et al.*, "Sub-250 fs passively mode-locked ultralong ring fibre oscillators," *Optics and Laser Technology*, vol. 138, p. 106848, Jun. 2021, doi: 10.1016/j.optlastec.2020.106848.
- [17] J. Limpert, F. Roser, T. Schreiber, and A. Tunnermann, "High-power ultrafast fiber laser systems," *IEEE Journal of Selected Topics in Quantum Electronics*, vol. 12, no. 2, pp. 233–244, Mar. 2006, doi: 10.1109/JSTQE.2006.872729.
- [18] A. Driessen, D. H. Geuzebroek, E. J. Klein, R. Dekker, R. Stoffer, and C. Bornholdt, "Propagation of short lightpulses in microring resonators: Ballistic transport versus interference in the frequency domain," *Optics Communications*, vol. 270, no. 2, pp. 217–224, Feb. 2007, doi: 10.1016/j.optcom.2006.09.034.
- [19] J.-C. Diels, "Ultrashort laser pulse phenomena," *Optical Engineering*, vol. 36, no. 8, p. 2362, Aug. 1997, doi: 10.1117/1.601465.
- [20] C. Gordon, M. Cumbajin, G. Carpintero, E. Bente, and J. Javaloyes, "Absorber length optimization of on-chip colliding pulse mode-locked semiconductor laser," *IEEE Journal of Selected Topics in Quantum Electronics*, vol. 24, no. 1, pp. 1–8, Jan. 2018, doi: 10.1109/JSTQE.2017.2759263.
- [21] C.-H. Lee and P. J. Delfyett, "Limits on amplification of picosecond pulses by using semiconductor laser traveling-wave amplifiers," *IEEE Journal of Quantum Electronics*, vol. 27, no. 5, pp. 1110–1114, May 1991, doi: 10.1109/3.83361.
- [22] J. Hillbrand *et al.*, "Mode-locked short pulses from an 8 μm wavelength semiconductor laser," *Nature Communications*, vol. 11, no. 1, p. 5788, Nov. 2020, doi: 10.1038/s41467-020-19592-1.
- [23] A. Pimenov, J. Javaloyes, S. V. Gurevich, and A. G. Vladimirov, "Light bullets in a time-delay model of a wide-aperture mode-locked semiconductor laser," *Philosophical Transactions of the Royal Society A: Mathematical, Physical and Engineering Sciences*, vol. 376, no. 2124, p. 20170372, Jul. 2018, doi: 10.1098/rsta.2017.0372.
- [24] G. P. Agrawal and N. A. Olsson, "Self-phase modulation and spectral broadening of optical pulses in semiconductor laser amplifiers," *IEEE Journal of Quantum Electronics*, vol. 25, no. 11, pp. 2297–2306, 1989, doi: 10.1109/3.42059.
- [25] A. Bednyakova, D. Khudozhitkova, and S. Turitsyn, "Nonlinear spectral tunability of pulsed fiber laser with semiconductor optical amplifier," *Scientific Reports*, vol. 12, no. 1, p. 13799, Aug. 2022, doi: 10.1038/s41598-022-17796-7.
- [26] A. Kokhanovskiy, E. Kuprikov, A. Bednyakova, I. Popkov, S. Smirnov, and S. Turitsyn, "Inverse design of mode-locked fiber laser by particle swarm optimization algorithm," *Scientific Reports*, vol. 11, no. 1, p. 13555, Jun. 2021, doi: 10.1038/s41598-021-92996-1.

- [27] S. Cuyvers, S. Poelman, K. V. Gasse, and B. Kuyken, "Hybrid modeling approach for mode-locked laser diodes with cavity dispersion and nonlinearity," *Scientific Reports*, vol. 11, no. 1, p. 10027, May 2021, doi: 10.1038/s41598-021-89508-6.
- [28] A. M. Perego, B. Garbin, F. Gustave, S. Barland, F. Prati, and G. J. de Valcárcel, "Coherent master equation for laser modelocking," *Nature Communications*, vol. 11, no. 1, p. 311, Jan. 2020, doi: 10.1038/s41467-019-14013-4.
- [29] J. C. Diels and W. Rudolph, *Ultrashort laser pulse phenomena: Fundamentals, techniques, and applications on a femtosecond time scale, second edition*, Elsevier, 2006.
- [30] D. C. Kirsch, A. Bednyakova, B. Cadier, T. Robin, and M. Chernysheva, "Gain-controlled broadband tuneability in mode-locked Thulium-doped fibre laser through variable feedback," *arXiv:2112.04799*, Dec. 2021.
- [31] C. Grill *et al.*, "Towards phase-stabilized Fourier domain mode-locked frequency combs," *Communications Physics*, vol. 5, no. 1, p. 212, Aug. 2022, doi: 10.1038/s42005-022-00960-w.

BIOGRAPHIES OF AUTHORS



Mubarak Hamad Oglah    has M.Sc. Degree in Physics from Mosul University in 1998 and 2001 also served as Faculty Member in the Department of Petroleum System Control Engineering in the College of Petroleum Processes Engineering, Tikrit University-Iraq. He has a Ph.D. in the field of quantum solid-state physics in Tikrit University. Currently activity is area of semiconductors and theoretical physics. He can be contacted at email: mubarak@tu.edu.iq.



Watban Ibrahim Mahmood    is a physics graduate who received his Master's degree in Physics from Tikrit University in 2019, specializing in Solid-State Physics (Semiconductors, Lasers, and Nanomaterials). He currently works as an Assistant Lecturer at Tikrit University, College of Al-Shirqat Eng. He is interested in writing papers to acquire the required knowledge and for the purpose of scientific advancement in semiconductors, applied physics, nanotechnology and medical physics, and renewable energy. He can be contacted at email: wa.ibraheem@tu.edu.iq.



Nawras Basheer Adday    a physics graduate, obtained his Master's degree in Solid-State Physics from Tikrit University in 2019. Currently, he serves as an Assistant Lecturer at Tikrit University's College of Engineering in Al-Shirqat. Nawras Basheer Adday's research interests encompass a diverse range of physics domains, including semiconductors, nanotechnology, and renewable energy. He can be contacted at email: nawras.adday21@tu.edu.iq.